Available online at www.sciencedirect.com

ScienceDirect

Ceramics International 39 (2013) 9369–9375

CERAMICS INTERNATIONAL

www.elsevier.com/locate/ceramint

Characteristics of aluminosilicates prepared from rice husk silica and aluminum metal

W. Simanjuntak[a], S. Sembiring[b], P. Manurung[b], R. Situmeang[a], I.M. Low[c,*]

[a]Department of Chemistry, Faculty of Mathematics and Natural Sciences, University of Lampung, Bandar Lampung 35145, Indonesia
[b]Department of Physics, Faculty of Mathematics and Natural Sciences, University of Lampung, Bandar Lampung 35145, Indonesia
[c]Department of Applied Physics, Curtin University, GPO Box U1987, Perth, WA 6845, Australia

Received 21 February 2013; received in revised form 30 April 2013; accepted 30 April 2013
Available online 29 May 2013

Abstract

This study investigated use of the electrochemical method to prepare aluminosilicates from rice husk silica and aluminum metal. The aluminosilicate precursors were characterized using Scanning Electron Microscopy/Energy Dispersive X-ray spectroscopy (SEM/EDX), Fourier Transform Infrared (FTIR) spectroscopy, and X-ray Diffraction spectroscopy (XRD). The precursors were subsequently sintered at 700–1400 °C and their microstructures and phase compositions were characterized. Results showed that the proposed method could be used to prepare aluminosilicates with high uniformity in terms of surface morphology and the particle size with mullite and quartz as the major phases formed.

Keywords: Rice husk; Silica; Aluminosilicates; Electrochemical method

1. Introduction

Aluminosilicate minerals with the basic formula of Al_2SiO_5 are composed of aluminum, silicon, and oxygen, in which some of the Si^{4+} ions are replaced by Al^{3+} ions in silicate to produce frameworks with Al–O–Si linkages. Many types of natural aluminosilicates are known, with different chemical compositions and crystal structures. These differences lead to varied physical characteristics, which make these minerals suitable for many industrial applications such as fabrication of glasses [1], ceramics [2], adsorbents [3], fuel cells [4], catalysts [5], building materials [6], and synthetic zeolites [7]. In recognition of the important roles of aluminosilicates mentioned above, the production of synthetic aluminosilicates from pure chemicals has been widely explored by many researchers all around the world. Synthetic aluminosilicates offer several advantages over natural aluminosilicates, which thus support a growing interest in this field. The use of pure chemicals as raw materials facilitates the production of purer and more uniform products, with a desirable composition and structure, which are not exhibited by natural aluminosilicates. This possibility offers an opportunity to produce aluminosilicates with the desired properties to suit specified applications. For instance, it was reported that aluminosilicates are promising acid catalysts [8]. Aluminosilicates have been applied as catalysts for alkylation of phenol with tert butanol [9] and for the production of dimethylether from methanol [5]. In addition, they have been used as adsorbents for organic dyes from aqueous solution [10], production of alumonosilicate-zeolite [11], and preparation of siliceous-zeolite membranes [12].

In the context of aluminosilicate synthesis, the choice of raw materials and optimization of experimental conditions have been the main focus of many studies. Currently, the sol–gel route is most commonly applied using various chemicals as the source of aluminum and silicon. Liu et al. [13] reported the synthesis of a typical hexagonal aluminosilicate mesostructure with the Si:Al ratio of 9:1 by mixing $NaAlO_2$ solution and sodium silicate solution, followed by acidification of the mixture using sulfuric acid to transform the mixture into a gel and aging of the gel produced for 20 h. In other studies [14,15], the synthesis of submicron-sized mesoporous aluminosilicate spheres

*Corresponding author. Tel.: +61 89 2667544; fax: +61 89 2662377.
E-mail address: low246@gmail.com (I.M. Low).

0272-8842/$ - see front matter
http://dx.doi.org/10.1016/j.ceramint.2013.04.112

was carried out using $Al_2(SO_4)_3$ solution and tetraethylorthosilicate (TEOS) as raw materials. The aluminosilicate gel was produced by dropwise addition of TEOS into $Al_2(SO_4)_3$ solution under stirring. The gel was then aged at room temperature for 16 h and dried at ambient temperature before being subjected to calcination treatment at 200 °C for 4 h. Several other studies have reported the synthesis of aluminosilicates from a variety of raw materials, such as sodium silicate and aluminum nitrate [5], potassium metoxy silicate ($K_2O \cdot SiO_2$) and $Al(NO_3)_3$ [16], Al $(NO_3)_3$ and TEOS [17], and sodium silicate and sodium aluminate [18].

The present study was carried out with the aim of exploring the feasibility of using the electrochemical method to produce aluminosilicate precursors from rice husk silica and aluminum metal as an alternative to commonly used aluminum salts. The precursor produced was then subjected to thermal treatment to investigate the phase development of aluminosilicate from the precursor. Rice husk silica was chosen because of the high availability of rice husk as an agriculture residue, which makes it a cost effective alternative as silica source. In addition, the potential of rice husk was investigated in recognition of its high silica content [19,20] and the solubility of the silica in alkaline solution, thus enabling the production of rice husk silica in the form of sols.

In this study, an electrochemical method was applied to produce aluminum ions since aluminum metal is known as a reactive electrode, with the standard oxidation potential of 1.66 V, and therefore could be electrochemically oxidized to produce Al^{3+} ions with relatively low potentials. In aqueous solution, the Al^{3+} ions produced by electrochemical oxidation of aluminum metal will react with water to produce various Al (III) species depending on the pH, the prominent species in alkaline condition being $Al(OH)_4^-$ [21,22]. In this study, the pH of the silica sol was 10.2, and therefore it is assumed that the Al(III) species present in the sample are $Al(OH)_4^-$ ions. Transformation of the mixture from sol to gel will promote the reaction between $Al(OH)_4^-$ and silica to produce the aluminosilicate precursor (hydroxyl-aluminosilicate) according to the following reaction [21].

$$(HO)_{4-x}SiO_x^{x-} + Al(OH)_4^- \rightarrow (HO)_3AlOSiO_x(OH)_{3-x}^{(x+1)-} + H_2O \quad (1)$$

The above equation clearly indicates that the quantity of hydroxyl-aluminosilicate formed is determined by the quantity of $Al(OH)_4^-$ available, which in turn depends on the quantity of Al^{3+} formed during the electrochemical process. In this respect, the amount of Al^{3+} ions produced by the electrochemical process is governed by the potential applied. Taking the role of this electrochemical variable into account, this study was carried out with a particular purpose to study the effect of oxidation potentials on the characteristics of the aluminosilicates precursors produced. Variation of potentials was considered as a base to choose the suitable potential for production of the most homogeneous precursor to be subjected to sintering treatment at different temperatures to study phase development of the aluminosilicate. In this regard, the experiments were conducted at different potentials of 4, 6, and 8 V for a fixed time of 30 min. The selected sample was then subjected to sintering treatment at different temperatures of 700, 850, and 1400 °C, and then characterized using X-ray diffraction and scanning electron microscopy.

2. Experimental details

2.1. Materials and instruments

Potassium hydroxide and hydrochloric acid used are reagent grade chemicals obtained from Merck. Two aluminum rods and two graphite rods were used as anodes and cathodes, respectively. Rice husks were obtained from the local rice milling industry. Before use, the husks were soaked in distilled water overnight for cleaning to remove the dirt, followed by oven drying at 110 °C overnight. Characteristics of the aluminosilicate were studied using SEM/EDX (Philips-XL), FTIR (Perkin Elmer spectrometer), and XRD (Shimadzu XD-610 diffractometer). A Nabertherm electrical furnace was used for heat-treating the samples.

2.2. Procedure

Rice husk silica was obtained using an alkali extraction method reported in literatures [19,23]. Typically, a sample of 50 g dried husk was mixed with 500 ml of 5% KOH solution in a beaker glass. The mixture was boiled for 30 min, and then allowed to cool to room temperature and left for 24 h. The mixture was filtered through a millipore filter to separate the filtrate which contains silica (silica sol). To obtain solid silica, the sol was acidified by dropwise addition of 10% HCl solution until the sol was converted into gel. The gel was aged for three days, and then rinsed repeatedly with de-ionized water to remove the excess of acid. The gel was oven dried at 110 °C for eight hours and ground into powder. A specified amount of silica powder was re-dissolved in 5% KOH solution to obtain silica sol as a sample for the electrochemical process.

Preparation of aluminosilicate was carried out using an electrochemical apparatus which consists of a home-made glass container with a cover having four drilled holes for assembling the electrodes. Four electrodes were used, two graphite rods as cathode and two aluminum rods as anode. The electrodes were fixed on the cover and inserted vertically into the cell at a distance of 2 cm from each other, with a 3 cm distance between the bottom of the electrodes and the bottom of the cell to allow easy stirring of the sample during the experiment. The cell was then connected to a variable voltage supply to allow the conduct of experiments at different potentials. To commence the experiment, an aliquot of 200 mL of silica sol was poured into the cell, and the potential was adjusted to a specified value. Electrolysis was carried out for 30 min, during which the sample was constantly stirred to promote distribution of Al^{3+} ions produced into the silica matrix. The experiments were carried out at potentials of 4, 6, and 8 V.

After the completion of the experiment, the sample was transferred into the beaker glass. The sample was acidified by dropwise addition of HCl solution (10%) to transform the sample into gel, followed by overnight aging of the gel. The gel was then oven dried at 110 °C for 8 h to produce dry solid aluminosilicate precursor, followed by grinding, and the ground powder was subjected to sintering at 700, 850 and 1400 °C, at a heating rate of 5 °C/min and holding time of 6 h at peak temperatures.

2.3. Characterization

Microstructural and elemental analysis was conducted using SEM/EDX Philips-XL, on polished and thermally-etched samples. The functionality of the sample was investigated using a Perkin Elmer FTIR spectrometer. The sample was ground with KBr of spectroscopy grade, and scanned over the wave number range of 4000–400 cm^{-1}. Powder XRD patterns were recorded to analyze phase development of aluminosilicate in order to gain information regarding the effect of sintering temperatures. The samples were examined using an automated Shimadzu XD-610 X-ray diffractometer. The operating conditions used were CuKα radiation (λ=1.5418 Å), produced at 40 kV and 30 mA, with a 0.15° receiving slit. Patterns were recorded over goniometry (2θ) ranges from 10° to 90° with a step size of 0.02, and using a post-diffraction graphite monochromator with a NaI detector. The diffraction data were analyzed using the JADE software after subtracting background and stripping the CuKα2 pattern [24].

3. Results and discussion

3.1. Characteristics of aluminosilicate precursors

As previously stated, the preparation of aluminosilicate precursor was carried out using three different potentials. To evaluate the effect of potentials on the surface morphology, the three samples were characterized using SEM/EDX. The micrographs produced with the magnification of 20,000 are shown in Fig. 1, and the corresponding EDX spectra are presented in Fig. 2. By visual inspection of the micrographs it can be seen that the effect of potential on the particle size and the homogeneity of the surface is quite evident. The sample prepared using the potential of 4 V (Fig. 1a) is characterized by the existence of particles with different sizes, indicating the presence of silica and Al(III) species. In this particular sample, the prominent particles are most likely the silica present as larger particles with gray color, suggesting that the sample is dominated by the silica. The presence of aluminum species distributed in the silica matrix is indicated by the existence of smaller particles with a bright color. This feature of heterogeneous morphology suggests that the Al^{3+} ions produced from the anodic oxidation of the Al metal anodes were insufficient to mix homogeneously with the silica, considering the standard oxidation potential of aluminum is 1.66 V, whereas the process was carried out in a non-standard condition.

Increasing the potential to 6 V was found to result in significantly different features when compared to that observed for the sample prepared using the potential of 4 V. As can be seen in Fig. 1b, the surface of this sample is characterized by smaller particle size and more homogeneous distribution of aluminum species within the silica matrix as a result of increased number of Al^{3+} ions produced with higher applied electrochemical potential. This feature also indicates that the aluminum species incorporated homogeneously within the silica, since the Al^{3+} ions are able to form chemical bonds with the silanol groups of silica molecules.

When the potential was increased further to 8 V (Fig. 1c), the sample was marked by the formation of clusters of different sizes. Formation of clusters in this sample is most likely due to agglomeration of aluminum species as a result of further increases in the amount of Al^{3+} ions during the electrochemical process. The results of SEM analyses clearly indicate that the most homogeneous sample was produced using the potential of 6 V. The results obtained from SEM analyses are supported by the composition of the samples as indicated by the EDX results shown in Fig. 2. The EDX data presented in Fig. 2 clearly indicated the siginificant effect of potentials on the composition (Al/Si ratio) of the samples. As can be seen, the sample prepared at 4 V only contained a very small amount (1.03%) of Al, and the percentage of this element increased sharply to 25.22% in the sample prepared at 6 V and to 25.43% in the sample prepared at 8 V. In terms of the Al/Si ratio, no significant difference between the samples prepared at the potential of 6 and 8 V was observed. However, the surface morphology of the samples as seen by SEM indicates that the sample prepared using the potential of 6 V is more homogeneous and possesses smaller particle sizes.

Fig. 3 shows the infrared spectra of the samples prepared with different potentials. The spectra of the samples are practically similar, suggesting that the three samples contain

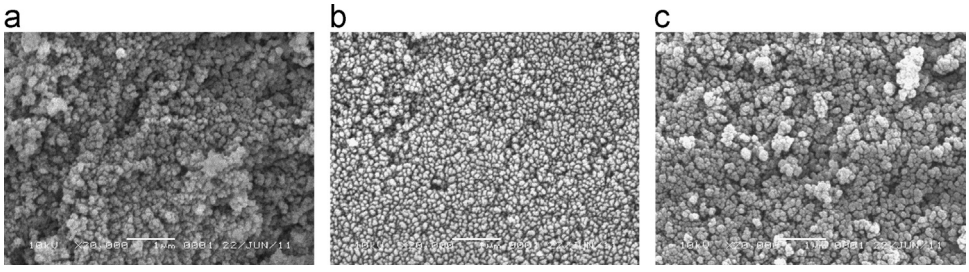

Fig. 1. Micrographs of the samples prepared using the potentials of (a) 4, (b) 6 and (c) 8 V.

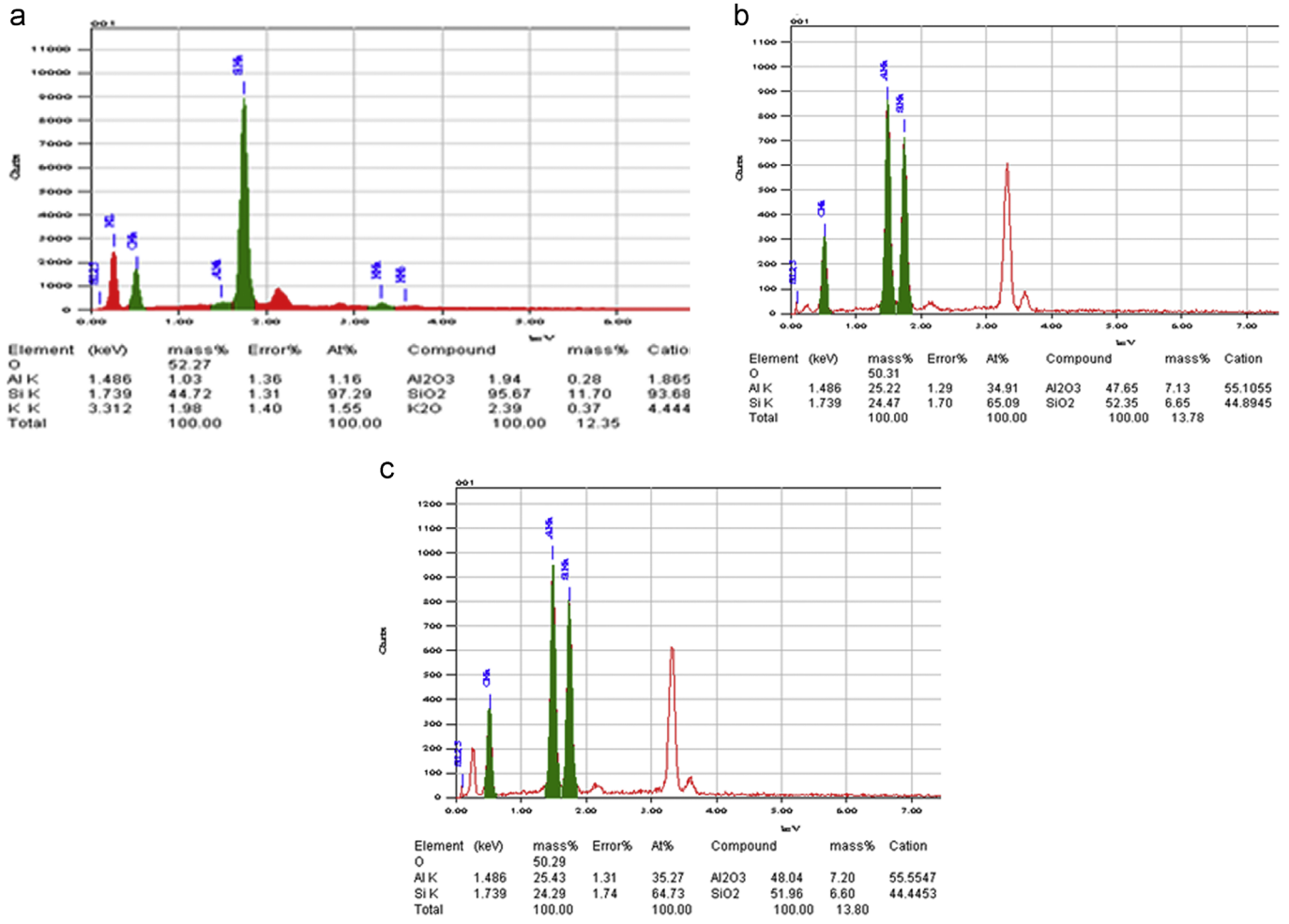

Fig. 2. The EDX spectra of the samples prepared at different potentials, a=4 V, b=6 V, and c=8 V.

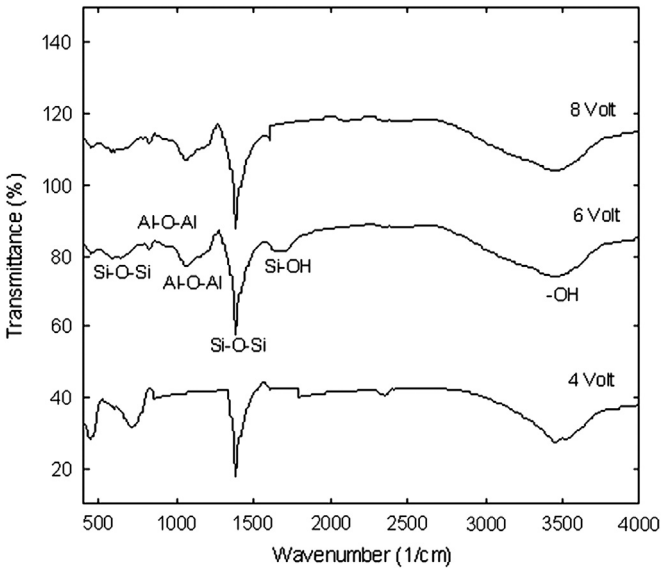

Fig. 3. FTIR spectra of aluminosilicate precursors prepared using different potentials.

the same functional groups. The most obvious peak is located at 3454 cm^{-1}, which is commonly assigned to stretching vibration of O–H bond in silanol group and water molecule. The contribution of water is confirmed by the presence of absorption band at 1647 cm^{-1} [20,25], as a result of bending vibration of the H–OH bond. The presence of peaks associated with O–H bond is most likely due to the presence of aluminum hydroxide species, $Si(OH)_4$, and trapped water. Two peaks located at 1383 and 468 cm^{-1} are commonly assigned to stretching vibration of Si–O–Si, and 803 and 1068 cm^{-1} to vibration of Al–O–Al, suggesting that some of the $Si(OH)_4$ and aluminum hydroxide were converted into their corresponding oxides.

The three samples were further characterized using XRD. This characterization was carried out to evaluate the crystallographic structure of the sample in order to get more insight into the formation of aluminosilicate moiety and to ascertain whether the sample was of amorphous or crystalline phase. The XRD patterns of the samples are shown in Fig. 4

As can be seen, the diffraction patterns presented in Fig. 4 indicate that the samples are essentially amorphous, marked by the existence of a broad peak at 2θ in the range of 20–35°, which is attributable to amorphous silica and aluminosilicate [26]. This suggests that silica and Al(III) species existed as hydrogel, which is supported by the presence of hydroxyl groups in the FTIR spectrum (Fig. 3). This finding is in good agreement with the existence of $Al(OH)_4^-$ gel and

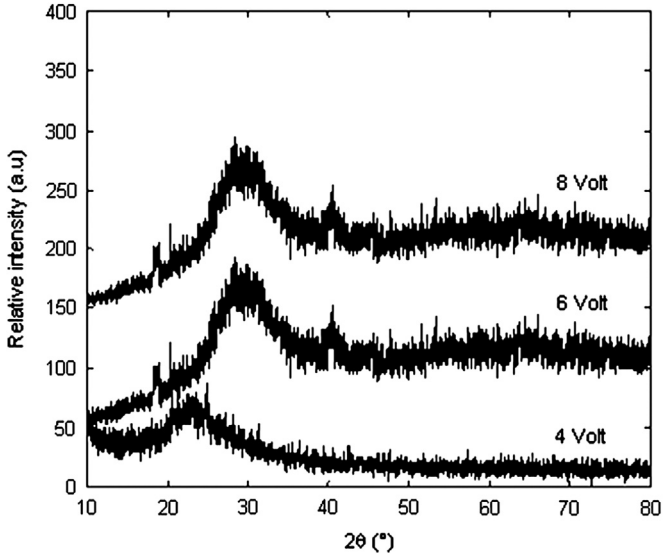

Fig. 4. The X-ray diffraction patterns of the aluminosilicate precursors prepared using different potentials.

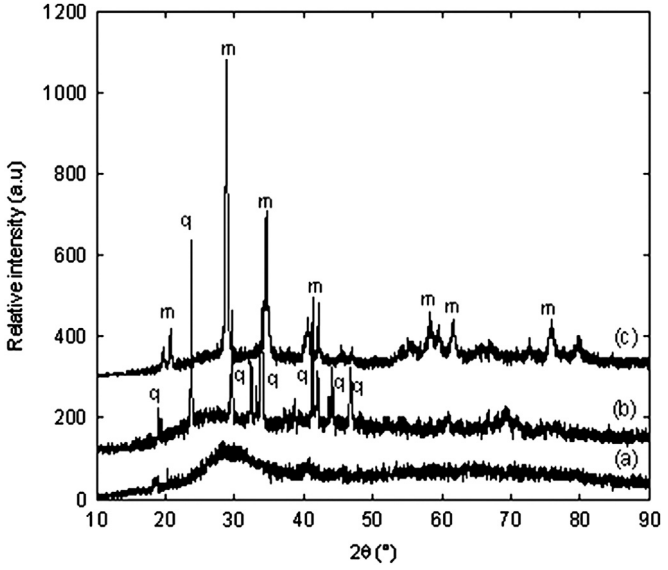

Fig. 5. The X-ray diffraction patterns of the samples prepared using the potential of 6 V sintered at different temperatures: (a) 700, (b) 850 and (c)1400 °C. Legend: m = mullite, and q = quartz.

amorphous silica at lower temperature as suggested by others [15]. These results confirmed that the samples are composed of $Al(OH)_4^-$ species and silica, therefore possess the potential as aluminosilicate precursor.

The surface morphology of the samples as seen by SEM indicates that the sample prepared using the potential of 6 V is more homogeneous and possesses smaller particle sizes. For these reasons, further investigation was focused on this particular sample, by subjecting the sample to sintering treatment at 700, 850, and 1400 °C, followed by characterization using SEM and XRD.

3.2. Phase development studies

To examine the phase development, the sintered sample at 700, 850, and 1450 °C were characterized using XRD and SEM. The XRD patterns obtained are shown in Fig. 5, in which the phases were identified with the aid of PDF diffraction lines using the search-match method [27].

The diffraction patterns in Fig. 5 indicate that the sample sintered at 700 °C was still amorphous, marked by the existence of a broad peak, most likely resulted from accumulation of small amounts of silicon oxide, aluminosilicate, and aluminum oxide. These phases were proposed based on the findings of others [28], who described the formation of γ-alumina and crystoballite in the aluminosilicate sample prepared from $AlCl_3$ and TEOS using sol–gel technique. Formation of crystalline phases was observed for samples sintered at higher temperatures. In the sample sintered at 850 °C (Fig. 5b), three phases were identified. The first phase is quartz, which is indicated by the most intense peak at $2\theta = 25.2^\circ$ (PDF-46-1045), the second phase is mullite with the most intense peak at $2\theta = 28.2^\circ$ (PDF-15-0776), and the last peak is alumina with the most intense peak at $2\theta = 34.9^\circ$ (PDF-46-1212). Detection of quartz and alumina demonstrates that at 850 °C, significant transformation of amorphous rice husk silica and aluminum hydroxide has taken place, and some of the quartz and alumina reacted to produce metastable mullite phase, as has also been reported by others [29,30]. When the sintering temperature was further increased to 1400 °C (Fig. 5c) a substantial change in crystallinity of the sample was observed, as characterized by a sharp increase of mullite phase and diminishing of quartz as well as alumina phase, suggesting that both quartz and alumina have completely transformed into mullite. In previous studies [29–32], it has been reported that at temperature at around 1400 °C, quartz was converted into liquid silica which penetrated alumina grain aggregates, and the two reacted to produce mullite. This is in good agreement with this study where mullite was the major phase present at 1400 °C.

The mean crystallite sizes (L) of mullite and quartz were calculated from the highest peaks for each phase using the Scherrer equation [33]:

$$L = \frac{K\lambda}{\beta \cos\theta} \quad (2)$$

where k is the shape factor (0.94), λ is the X-ray wavelength, β is the line broadening at full width at half maximum (FWHM) in radians, and θ is the Bragg angle. The corresponding crystallite size calculated from the Scherrer equation are 30 nm for mullite in the sample sintered at 1400 °C and 50 nm for quartz in then sample sintered at 850 °C. However, it should be acknowledged that the values of crystallite size are only relative because the contribution of strain on peak broadening has been ignored in the calculation.

Fig. 6 shows microstructures of samples after they were subjected to sintering at different temperatures, revealing quite significant effect of sintering temperature on the surface morphology. A comparison of the sample sintered at 700 °C with the unsintered sample (Fig. 1b) shows that sintering led to agglomeration of the aluminum oxide particles. This process resulted in separation of aluminum oxide agglomerates from

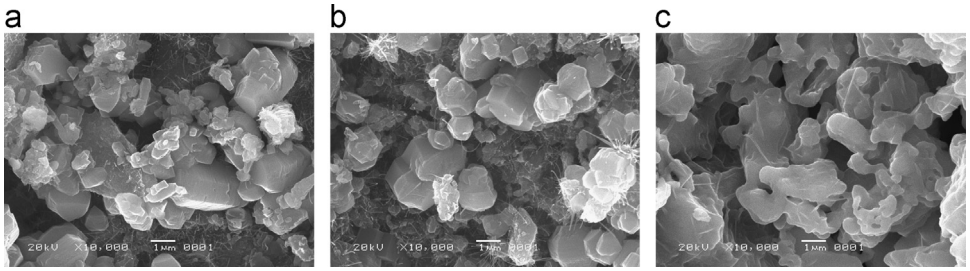

Fig. 6. SEM images showing the microstructures of samples sintered at different temperatures: (a) 700, (b) 850 and (c) 1400 °C.

silica agglomerates, producing clusters of different shapes and sizes (Fig. 6a) in amorphous state as evidently displayed by the XRD pattern of the sample (Fig. 5a). The microstructure of the sample sintered at 850 °C was characterized by the existence of larger grains with different shapes, indicating that increased temperature intensified the agglomeration of the particles separated by grain boundaries. As seen by the XRD, this sample is characterized by the existence of quartz and small amount of mullite. This suggests that at this temperature, the siliceous phase has started to melt and reacted with alumina aggregates to form mullite. The microstructure of sample sintered at 1400 °C displays very uniform grains with smooth surface and without clear grain boundaries. The existence of granular microstructure with smooth surface suggests that at this temperature the quartz had converted into liquefied silica which penetrated the alumina aggregates, thus intensifying the formation of mullite as supported by the XRD results (Fig. 5c), in which the only phase detected is mullite.

4. Conclusions

The present work demonstrates that it is possible to prepare aluminosilicate precursors by using the electrochemical method from rice husk silica and aluminum metal to replace the commonly used raw materials. Overall, the results demonstrate that the aluminosilicate precursor with high uniformity in terms of surface morphology and the particle size could be obtained using the proposed method. Characterization of samples using XRD and SEM shows that the precursor synthesized could be transformed into mullite at 1400 °C, thus suggesting that the electrochemical method is a promising technique for producing aluminosilicate materials.

References

[1] A. Gritco, M. Moldovan, R. Grecu, V. Simon, Thermal and infrared analyses of aluminosilicate glass systems for dental implants, Journal of Optoelectronics and Advanced Materials 7–6 (2005) 2845–2847.
[2] F. Ye, S. Chen, M. Iwasa, Synthesis and properties of barium aluminosilicate glass–ceramic composites reinforced with in situ grown Si_3N_4 whiskers, Scripta Materialia 48 (2003) 1433–1438.
[3] S.A. El-Safty, A. Shahat, M.E. Awual, Efficient adsorbents of nanoporous aluminosilicate monoliths for organic dyes from aqueous solution, Journal of Colloid and Interface Science 1 (2011) 9–18.
[4] N. Lahl, D. Bahadur, K. Singh, L. Singheiser, K. Hilpert, Chemical interactions between aluminosilicate base sealants and the components on the anode side of solid oxide fuel cells, Journal of the Electrochemical Society 149 (2002) A607–A614.
[5] D. Varisli, K.C. Tokaya, A. Ciftci, T. Dogu, G. Dogu, Methanol dehydration reaction to produce clean diesel alternative dimethylether over mesoporous aluminosilicate-based catalysts, Turkish Journal of Chemistry 33 (2009) 355–366.
[6] C.H. Ruscher, E.M. Mielcarek, J. Wongpa, C. Jaturapitakkul, F. Jirasit, L. Lohaus, Silicate, aluminosilicate and calciumsilicate gels for building materials: chemical and mechanical properties during ageing, European Journal of Mineralogy 23 (2010) 111–124.
[7] S. Shevade, R.G. Ford, Use of synthetic zeolites for arsenate removal from pollutant water, Water Research 38 (2004) 3197–3204.
[8] J. Pinkas, Chemistry of silicates and aluminosilicates, Ceramics-Silikáty 49 (4) (2005) 287–298.
[9] L. Xu, S. Wu, J. Guan, Yu. Ma, K. Song, H. Xu, C. Xu, Z. Wang, Q. Kan, Synthesis, characterisation and catalytic activity of a novel mesoporous aluminosilicate catalyst by a citric acid route, Catalysis Communications 9 (2008) 1970–1973.
[10] S.A. El-Safty, A. Shahat, M.D. Awual, Efficient adsorbents of nanoporous aluminosilicate monoliths for organic dyes from aqueous solution, Journal of Colloid and Interface Science 359 (2011) 9–18.
[11] A. Farouq Twaiq, M. Noor Asmawati, M. Zabidi, A.R. Mohamed, S. Bhatia, Catalytic conversion of palm oil over mesoporous aluminosilicate MCM-41 for the production of liquid hydrocarbon fuels, Fuel Processing Technology 84 (2003) 105–120.
[12] M. Pan, Y.S. Lin, Template-free secondary growth of MFI type zeolite membranes, Microporous and Mesoporous Materials 43 (2001) 217–219.
[13] Y. Liu, W. Zhang, T.J. Pinnavaia, Steam-stable aluminosilicate mesostructures assembled from zeolite type Y seeds, Journal of the American Chemical Society 122 (2000) 8791–8792.
[14] G. Gundiah, M. Moorthy, S. Neeraj, S. Natarajan, C.N.R. Rao, Synthesis and characterization of submicron-sized mesoporous aluminosilicate spheres, Proceedings of the Indian Academy of Sciences (Chemical Science) 113 (3) (2001) 227–234.
[15] D.A. de Haro-Del Rio, A.F. Aguilera-Alvarado, I. Cano-Aguilera, M. Martinez-Rosales, S. Holmes, Synthesis and characterisation of mesoporous aluminosilicates for copper removal from aqueous medium, Materials Sciences and Applications 3 (2012) 485–491.
[16] F. Jiménez, R. Ramesh Vallepu, T. Tohru Terai, A. Palomo, K. Ikeda, Synthesis and thermal behaviour of different aluminosilicate gels, Journal of Non-Crystalline Solids 352 (2006) 2061–2066.
[17] S.R. Zhai, I. Kim, C.S. Ha, Structural and catalytic characterization of nanosized mesoporous aluminosilicates synthesized via a novel two-step route, Catalysis Today 131 (2008) 55–60.
[18] Y.S. Lin, H.P. Lin, C.Y. Mou, A simple synthesis of well-ordered supermicroporous aluminosilicate, Microporous and Mesoporous Materials 76 (2004) 203–208.
[19] A.A.M. Daifullah, N.S. Awwad, S.A. El-Reefy, Purification of wet phosphoric acid from ferric ions using modified rice husk, Chemical Engineering and Processing 43 (2004) 193–201.
[20] G. Irwan, W. Simanjuntak, D.P. Kamisah, Potential utilization of rice husk silica as an alternative for mineral derived silica, in: Proceedings of the International Seminar on Sustainable Biomass Production and Utilization: Challenges and Opportunity, The University of Lampung, 2009, pp. 396–402.
[21] T.W. Swaddle, Silicate complexes of aluminum (III) in aqueous systems, Coordination Chemistry Reviews 219 (2001) 665–686.

[22] P.K. Holt, G.W. Barton, M. Wark, C.A. Mitchell, A quantitative comparison between chemical dosing and electrocoagulation, Colloids and Surfaces A: Physicochemical and Engineering Aspects 211 (2002) 233–248.
[23] S. Sembiring, Synthesis and characterization of rice husk silica based borosilicate (B_2SiO_4) ceramics by sol–gel routes, Indonesian Journal of Chemistry 11 (2011) 85–89.
[24] JADE Program XRD Pattern Processing PC, Material Data Inc (MDI), Livermore, CA, 1997.
[25] F. Adam, J.H. Chua, The adsorption of palmytic acid on rice husk ash chemically modified with Al(III) ion using the sol–gel technique, Journal of Colloid and Interface Science 280 (2004) 55–61.
[26] J. Temuujin, Characterisation of aluminosilicate (mullite) precursors prepared by a mechanochemical process, Journal of Materials Research 13 (1998) 2184–2188.
[27] Powder Diffraction File (Type PDF-2), Diffraction Data for XRD Identification, International Centre for Diffraction Data, PA, USA, 1997.
[28] H.S. Hong, G.I. Messing, Anisotropic grain growth in diphasic-gel derived titania-doped mullite, Journal of the American Ceramic Society 81 (1998) 1269–1277.
[29] H.J. Kleebe, F. Siegelin, T. Straubinger, G. Ziegler, Conversion of Al_2O_3–SiO_2 powder mixtures to 3:2 mullite following the stable or metastable phase diagram, Journal of the European Ceramic Society 21 (2001) 2521–2533.
[30] S. Sembiring, W. Simanjuntak, X-Ray diffraction phase analysis of mullite derived from rice husk silica, Makara Journal of Science 16 (2) (2012) 77–82.
[31] M.D. Sacks, K. Wang, G.W. Scheiffele, N. Bozkurt, Effect of composition on mullitisation behavior of α-alumina/silica micro composite powder, Journal of the American Ceramic Society 80 (3) (1997) 663–672.
[32] P. Nampi Padmaja, Moothetty Padmanabhan, F. Berry, M. John, G. Michael, Warrier Krishna, Aluminosilicates with varying alumina–silica ratios: synthesis via a hybrid sol–gel route and structural characterization, DaltonTransactions 39 (2010) 5101–5105.
[33] B.D. Cullity, S.R. Stock, Elements of X-ray Diffraction, 3rd ed., Prentice-Hall Inc., Englewood Cliffs, NJ167.